

# Recent Advances in Beam Focusing through Resonant Bessel-Beam Launchers for Millimeter-Wave WPT Applications

Edoardo Negri<sup>1\*</sup>, Francesca Benassi<sup>2†</sup>, Walter Fuscaldo<sup>3‡</sup>, Diego Masotti<sup>4†</sup>,  
Paolo Burghignoli<sup>5\*</sup>, Alessandra Costanzo<sup>6†</sup>, Alessandro Galli<sup>7\*</sup>

<sup>\*</sup>Department of Information Engineering, Electronics and Telecommunications, Sapienza University of Rome, Rome, Italy, {edoardo.negri<sup>1</sup>, paolo.burghignoli<sup>5</sup>, alessandro.galli<sup>7</sup>}@uniroma1.it

<sup>†</sup>Department of Electrical, Electronic, and Information Engineering “Guglielmo Marconi”, University of Bologna, Bologna, Italy, {francesca.benassi<sup>9</sup>, diego.masotti<sup>4</sup>, alessandra.costanzo<sup>6</sup>}@unibo.it

<sup>‡</sup>Istituto per la Microelettronica e Microsistemi, Consiglio Nazionale delle Ricerche, Rome, Italy, walter.fuscaldo@cnr.it

**Abstract**—Resonant Bessel-beam launchers have recently gained much attention due to their capability to radiate focused beams by means of a compact and low-cost devices at microwave and/or millimeter waves. Most realizations consider only the use of TM-polarized beams, whereas only few works deal with the TE case. Here, we present an original workflow based on leaky-wave theory for the design and performance analysis of both kinds of launchers in wireless power transfer (WPT) scenarios. Simple analytical formulas are provided and validated with both numerical and full-wave methods for different case studies. The results obtained here offer considerable insight into the WPT performance of such devices.

**Index Terms**—Bessel beams, near-field focusing, leaky waves, wireless power transfer

## I. INTRODUCTION

Different modern applications, such as high data-rate transfer [1] and medical imaging [2], just to name but a few, call for compact devices capable of radiating focused beams in the *radiative near field* at high frequencies.

As a matter of fact, radiative near-field links show a larger cover distance with respect to typical *reactive near-field links* based on inductive coupling [3] and a higher efficiency with respect to *far-field links* [4]. Moreover, the implementation of this kind of links at high frequencies allows for device miniaturization: a desirable feature in diverse practical applications, such as wireless power transfer (WPT) for wearable devices [5].

For the reasons above, the possibility to realize radiative near-field links at millimeter-waves through planar, low-profile, low-cost devices has recently gained much attention [6], [7]. In this context, resonant Bessel-beam launchers (BBLs) represent promising candidates due to their capability to radiate Bessel beams, by means of a metallic cavity which is a few wavelengths large and half-a-wavelength thick. Bessel beams are an attractive type of focused beams with self-healing properties, i.e. with the capability to reconstruct themselves after an obstacle [8]. In case of a low number of lobes, Bessel beams can also be preferred to the more localized Gaussian

beams thanks to their limited-diffraction behavior, i.e., their ability to maintain the transverse intensity beam distribution almost constant during the propagation [9].

More precisely, resonant BBLs are constituted by a dielectric-filled cylindrical metallic cavity whose upper face is replaced by a partially reflecting sheet (PRS). This resonant device is typically excited by a dipole-like source: a vertical electric dipole (VED) in case of a transverse magnetic (TM) polarized BBL (see, e.g., [10] or [11]) and a vertical magnetic dipole (VMD) for a transverse electric (TE) polarized BBL [12]. However, resonant TM-polarized BBLs are way more common than TE-polarized BBLs, although the latter can be of interest for applications where the coupling with dielectric objects has to be minimized [12]. This scientific trend is justified by the practical implementation of a VED in the TM case. Indeed, a VED has a simple, practical, and low-cost implementation given by a coaxial probe. Conversely, typical implementations of VMDs are loop antennas and coils [12] that, due to their feeding structure, do not present an exact azimuthal symmetry and, thus, do not excite a purely TE-polarized field. Only recently, it has been shown [13] that a purely TE-polarized Bessel-beam can be conveniently excited through a radial slot array etched on the ground plane of the resonant BBL.

In this work, we aim at providing a simple and effective design workflow suitable for both kinds (viz. TM- and TE-polarized) of resonant BBLs with a description of a WPT link between them and its performance. The paper is organized as follows. In Section II, an efficient leaky-wave approach is exploited in order to describe and design differently polarized BBLs. In Section III, a radiative near-field WPT link is realized through two identical resonant BBLs and its performance is rigorously evaluated [14]. In Section IV, conclusions are drawn.

## II. THEORETICAL APPROACH

The common architecture of resonant BBLs consists of a circular metallic rim around a grounded dielectric slab with a

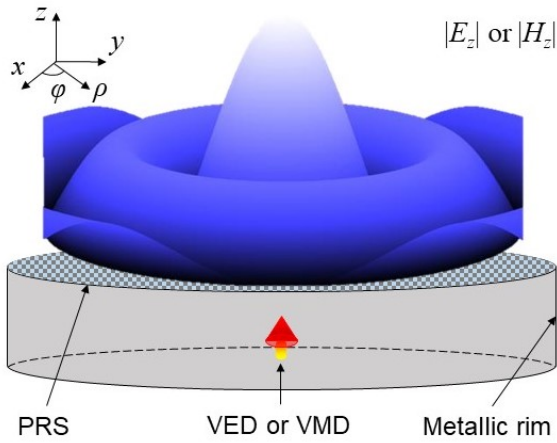


Fig. 1. Pictorial representation of a resonant BBL and of its theoretical near-field distribution:  $|E_z|$  or  $|H_z|$  for a TM- or a TE-polarized case, respectively.

PRS on top [15], as shown in Fig. 1. This defines a partially open circular cylindrical cavity, whose main design parameters are: the thickness of the dielectric slab  $h$  (or, the cavity height in the air-filled case), the radius of the circular metallic rim  $\rho_{\text{ap}}$ , and the surface reactance of the PRS  $X_s$ , which fully characterizes the electromagnetic response of canonical homogenized lossless metasurfaces, such as arrays of metallic patches, strip gratings, etc. [16].

The aperture radius  $\rho_{\text{ap}}$  and the working frequency  $f_0$  are typically set by practical constraints dictated by the application scenario. In a realistic implementation of a millimeter-wave radiative near-field WPT link for wearable devices, the working frequency has been set here to  $f_0 = 30$  GHz and the maximum aperture radius to  $\rho_{\text{ap}} = 15$  mm. The parameters  $h$  and  $X_s$  have then to be fixed in order to enforce the radial resonance of the desired Bessel-like beam as explained below.

In a TE(TM)-polarized BBL, a zeroth order BB distribution is theoretically excited over the vertical magnetic(electric) field component, as depicted in Fig. 1. Thanks to its limited-diffraction property, this field distribution is maintained up to a certain distance called *nondiffractive range*  $z_{\text{ndr}}$ . The  $z_{\text{ndr}}$  value is related to  $\rho_{\text{ap}}$  and the so-called axicon angle  $\theta_0$  through the following equation [11]:

$$z_{\text{ndr}} = \rho_{\text{ap}} \cot \theta_0. \quad (1)$$

In a resonant BBL, the axicon angle is strictly related to the phase constant  $\beta$  of the relevant leaky wave, i.e., the real part of its radial wavenumber  $k_p = \beta - j\alpha$  (being  $\alpha$  the attenuation constant), through the relation  $\beta = k_0 \sin \theta_0$ , because of the underlying leaky radiation mechanism (a rigorous explanation in terms of complex rays can be found in [17]), where  $k_0$  is the free-space wavenumber.

In order to excite the theoretical field distribution, the outward leaky wave generated from the source and the inward one reflected by the metallic rim should add in phase and with almost the same amplitude. Therefore, two different conditions have to be satisfied: an amplitude condition described by the

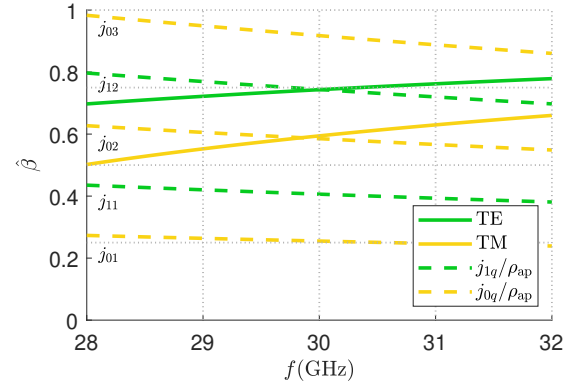


Fig. 2. Dispersion diagrams for TE and TM modes representing the normalized phase constant  $\hat{\beta}$  vs. frequency  $f$ . Green and yellow dashed lines represent the radial resonances of the device for TE and TM modes, respectively. Green and yellow solid lines are the dispersion curves of the higher-order TE and TM leaky modes propagating in the cavity, respectively.

attenuation constant  $\alpha$ , and a phase condition given by the radial resonance enforced by the phase constant  $\beta$ .

The normalized attenuation constant  $\hat{\alpha} = \alpha/k_0$  has to be determined in order to obtain almost the same power amplitude for outward and inward cylindrical waves. By applying a plane-wave approximation and by considering a minimum power ratio between the waves equal to 0.95, the upper bound for the normalized attenuation constant is set to  $\hat{\alpha} = 0.0027$ .

The normalized phase constant  $\hat{\beta} = \beta/k_0$  has to be fixed in order to enforce the correct radial resonance, which however depends on the polarization type. In particular, different boundary conditions have to be applied according to the polarization type: the circular metallic rim has to be placed at a radial distance from the central feeder which coincides with one of the nulls of the zeroth-order (first-order) Bessel function for the TM (TE) case (see, e.g., [11] and [18]). Therefore, the normalized phase constant should satisfy the following condition:

$$\hat{\beta} = \frac{j_{nq}}{k_0 \rho_{\text{ap}}}, \quad (2)$$

where  $j_{nq}$  is the  $q$ -th zero of the  $n$ -th order Bessel function, with  $n = 0$  and  $n = 1$  for the TM and TE case, respectively. For  $q = 2$ ,  $\hat{\beta} = 0.5857$  and  $\hat{\beta} = 0.7436$  corresponding to  $z_{\text{ndr}} \simeq 20$  mm and  $z_{\text{ndr}} \simeq 13.5$  mm are found for the TM- and TE-polarized resonant BBL, respectively.

Once the  $\hat{\alpha}$  and  $\hat{\beta}$  values have been fixed and an air-filled cavity is considered in order to reduce dielectric losses, the remaining design parameters of a resonant BBL  $X_s$  and  $\rho_{\text{ap}}$  are found as shown in [19], and are reported in Table I. It is worth noting that is possible to consider a dielectric-filled cavity instead of an air-filled one in order to reduce the vertical extension of the devices at the expense of dielectric losses.

The accuracy of this choice of parameters can be inferred from Fig. 2, where the dispersion curves of both the TE and TM leaky modes are reported along with the radial resonance given by  $\beta \rho_{\text{ap}} = j_{nq}$  for both polarizations and  $q = 1, 2, 3$ .

TABLE I  
PARAMETERS FOR TE- AND TM-POLARIZED BBLs WORKING WITH THE  
2<sup>nd</sup> RADIAL RESONANCE AND AN APERTURE RADIUS OF 15 MILLIMETERS

Polarization	$X_s$ [ $\Omega$ ]	$h$ [mm]	$z_{\text{ndr}}$ [mm]
TE	67.2	7.19	13.5
TM	26.7	6.04	20

The intersections between the  $q = 2$  radial resonances and  $\hat{\beta}$  yield the working points for the TM and TE cases at  $f_0 = 30$  GHz, as expected. Further details about the dispersion curves analysis can be found in [11].

Once the design parameters have been found, it only remains to effectively excite TE or TM modes inside the cavity. As commented in the Introduction, while VEDs are well realized in practice by means of coaxial probes, it does not hold the same for VMDs with loop antennas or coils (see, e.g., [20]). However, in order to limit the TM components due to the asymmetry introduced by the feeding point of the loop-antenna source, an interesting annular strip grating metasurface has been exploited in [20] obtaining a *hybrid* TE-polarized BBL. It has recently been shown in [13] that a purely TE-polarized BBL can be excited by means of a radial slot array on the ground plane, which is the discrete counterpart of a radially directed magnetic surface current. In the next section, all the devices presented in [20] and [13] are exploited in order to realize radiative near-field WPT links and their performance is evaluated.

### III. RADIATIVE NEAR-FIELD WPT LINKS

A radiative near-field WPT link can be realized with two resonant BBLs placed one in front of the other, as shown in Fig. 3. A rigorous and efficient approach to evaluate the WPT performance is exploited [14].

In this model, the entire WPT link performance is obtained from just one full-wave simulation of the transmitting (TX) side through CST Microwave Studio [21], thus halving the computational time of the overall connection. The simulated electromagnetic field of the TX side can be extracted on a plane  $S$ , placed exactly in the middle of the separation distance between the TX launcher and the receiving (RX) one. By exploiting the reciprocity theorem and the equivalence theorem on  $S$ , as shown in [14], the equivalent current  $I_{\text{eq}}$  of the RX Norton's equivalent circuit can be found. By obtaining the antenna admittance  $Y_a(f)$  through full-wave simulations, the received power has been obtained for the conjugated match case:

$$P_r = \frac{|I_{\text{eq}}|^2}{8\text{Re}[Y_a(f)]} \quad (3)$$

A comparison between the WPT performance of differently polarized BBLs can be done by considering three different links between two TE-polarized BBLs, two TM-polarized BBLs, and two hybrid-TE polarized BBLs. By considering different distances between the TX and RX devices (namely, 20, 30, and 40 mm) and a transmitting power equal to 21 dBm, the received power for each polarization is reported in Fig. 4.

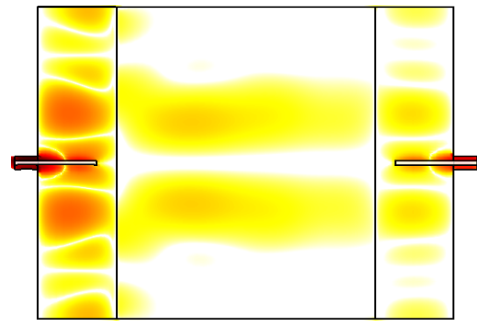


Fig. 3. Real part of the vertical component of the Poynting vector  $\Pi_z$  obtained through a full-wave simulation of the TM-polarized WPT link at 20 cm. The  $\text{Re}(\Pi_z)$  distribution is reported through a contour plot with a color map that goes from white (20 dB(W/m<sup>2</sup>)) to black (60 dB(W/m<sup>2</sup>)).

As expected, the resonant cases with TE or TM polarization show almost the same performance, also taking into account the lower nondiffractive range of the TE-polarized case. The hybrid-TE link, instead, shows an inferior performance.

### IV. CONCLUSION

In this work, a millimeter-wave wireless power transfer link is investigated between resonant Bessel-beam launchers operating in different polarization conditions. The design workflow of such kinds of devices is derived under a leaky-wave interpretation, whereas the link power budget is evaluated with a rigorous and fast method. Comparable and interesting results have been obtained for purely TE- or TM-polarized Bessel-beam launchers, whereas the hybrid-TE case has shown an inferior performance. Thanks to their limited sizes and their efficient power transmission at millimeter-waves, resonant Bessel-beam launchers represent an innovative yet effective solution for wireless power transfer applications. A theoretical analysis of the annular strip grating exploited in the hybrid TE case, the effect of a lossy material between the transmitting and receiving device, and the experimental validation of the obtained results will be addressed in future works.

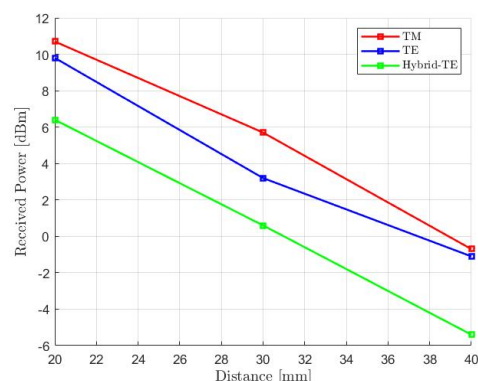


Fig. 4. Received power vs. distance in a radiative near-field WPT link realized through differently polarized BBLs.

## ACKNOWLEDGMENT

This work was funded by the Italian Ministry of Education, University and Research (MIUR) within the framework of the PRIN 2017-WPT4WID ('Wireless Power Transfer for Wearable and Implantable Devices') ongoing project.

## REFERENCES

- [1] S. Chen, S. Li, Y. Zhao, J. Liu, L. Zhu, A. Wang, J. Du, L. Shen, and J. Wang, "Demonstration of 20-Gbit/s high-speed Bessel beam encoding/decoding link with adaptive turbulence compensation," *Opt. Lett.*, vol. 41, no. 20, pp. 4680–4683, Oct 2016.
- [2] C. Liu, Z. Zhao, C. Jin, Y. Xiao, G. Gao, H. Xie, Q. Dai, H. Yin, and L. Kong, "High-speed, multi-modal, label-free imaging of pathological slices with a Bessel beam," *Biomed. Opt. Express*, vol. 11, no. 5, pp. 2694–2704, 2020.
- [3] V. R. Gowda, O. Yurduseven, G. Lipworth, T. Zupan, M. S. Reynolds, and D. R. Smith, "Wireless power transfer in the radiative near field," *IEEE Antennas Wirel. Propag. Lett.*, vol. 15, pp. 1865–1868, 2016.
- [4] J. Garnica, R. A. Chinga, and J. Lin, "Wireless power transmission: From far field to near field," *Proc. IEEE*, vol. 101, no. 6, pp. 1321–1331, 2013.
- [5] F. Benassi, W. Fuscaldo, D. Masotti, A. Galli, and A. Costanzo, "Wireless power transfer in the radiative near-field through resonant Bessel-beam launchers at millimeter waves," in *2021 IEEE Wireless Power Transf. Conf. (WPTC)*, San Diego, CA, USA, 2021, pp. 1–4.
- [6] M. Ettore, S. C. Pavone, M. Casaletti, M. Albani, A. Mazzinghi, and A. Freni, "Near-field focusing by non-diffracting Bessel beams," in *Aperture Antennas for Millimeter and Sub-Millimeter Wave Applications*. Cham, Switzerland: Springer, 2018, pp. 243–288.
- [7] E. Negri, W. Fuscaldo, P. Burghignoli, and A. Galli, "Leaky-wave analysis of TM-, TE-, and hybrid-polarized aperture-fed Bessel-beam launchers for wireless power transfer links," *IEEE Trans. Antennas Propag.*, Early Access 2022.
- [8] D. McGloin and K. Dholakia, "Bessel beams: diffraction in a new light," *Contemporary Phys.*, vol. 46, no. 1, pp. 15–28, 2005.
- [9] W. Fuscaldo, P. Burghignoli, and A. Galli, "A comparative analysis of Bessel and gaussian beams beyond the paraxial approximation," *Optik*, vol. 240, p. 166834, 2021.
- [10] D. Comite, W. Fuscaldo, S. K. Podilchak, P. D. Hilaro-Re, V. Gómez-Guillamón Buendía, P. Burghignoli, P. Baccarelli, and A. Galli, "Radially periodic leaky-wave antenna for Bessel beam generation over a wide-frequency range," *IEEE Trans. Antennas Propag.*, vol. 66, no. 6, pp. 2828–2843, Jun. 2018.
- [11] W. Fuscaldo, G. Valerio, A. Galli, R. Sauleau, A. Grbic, and M. Ettore, "Higher-order leaky-mode Bessel-beam launcher," *IEEE Trans. Antennas Propag.*, vol. 64, no. 3, pp. 904–913, Mar. 2016.
- [12] P. Lu, A. Bréard, J. Huillery, X.-S. Yang, and D. Voyer, "Feeding coils design for TE-polarized Bessel antenna to generate rotationally symmetric magnetic field distribution," *IEEE Antennas Wireless Propag. Lett.*, vol. 17, no. 12, pp. 2424–2428, Dec. 2018.
- [13] E. Negri, F. Benassi, W. Fuscaldo, D. Masotti, P. Burghignoli, A. Costanzo, and A. Galli, "Effective TE-polarized Bessel-beam excitation for wireless power transfer near-field links," in *52<sup>nd</sup> Europ. Microw. Conf. (EuMC 2022)*, Milan, IT, 2022, pp. 1–4.
- [14] V. Rizzoli, D. Masotti, N. Arbizzani, and A. Costanzo, "CAD procedure for predicting the energy received by wireless scavenging systems in the near- and far-field regions," in *2010 IEEE MTT-S Int. Microw. Symp.*, 2010, pp. 1768–1771.
- [15] E. Negri, W. Fuscaldo, P. Burghignoli, and A. Galli, "A leaky-wave analysis of resonant Bessel-beam launchers: Design criteria, practical examples, and potential applications at microwave and millimeter-wave frequencies," *Micromachines*, vol. 13, no. 12, p. 2230, 2022.
- [16] O. Luukkonen, C. Simovski, G. Granet, G. Goussetis, D. Lioubtchenko, A. V. Raisanen, and S. A. Tretyakov, "Simple and accurate analytical model of planar grids and high-impedance surfaces comprising metal strips or patches," *IEEE Trans. Antennas Propag.*, vol. 56, no. 6, pp. 1624–1632, Jun. 2008.
- [17] L. Felsen, "Real spectra, complex spectra, compact spectra," *JOSA A*, vol. 3, no. 4, pp. 486–496, 1986.
- [18] P. Lu, D. Voyer, A. Bréard, J. Huillery, B. Allard, X. Lin-Shi, and X.-S. Yang, "Design of TE-polarized Bessel antenna in microwave range using leaky-wave modes," *IEEE Trans. Antennas Propag.*, vol. 66, no. 1, pp. 32–41, Jan. 2017.
- [19] W. Fuscaldo, A. Galli, and D. R. Jackson, "Optimization of 1-D unidirectional leaky-wave antennas based on partially reflecting surfaces," *IEEE Trans. Antennas Propag.*, vol. 70, no. 9, pp. 7853–7868, Sep. 2022.
- [20] F. Benassi, W. Fuscaldo, E. Negri, G. Paolini, E. Augello, D. Masotti, P. Burghignoli, A. Galli, and A. Costanzo, "Comparison between hybrid- and TM-polarized Bessel-beam launchers for wireless power transfer in the radiative near-field at millimeter waves," in *51<sup>st</sup> Europ. Microw. Conf. (EuMC 2021)*, London, UK, 2022, pp. 1–4.
- [21] "CST products Darmstadt, Germany, 2019." [Online]. Available: <http://www.cst.com>